AN EXPERIMENT STUDY OF FRONTAL CYCLONES OVER THE WESTERN ATLANTIC OCEAN*

CUI Xiaopeng (崔晓鹏), *WU Guoxiong* (吴国雄) and *GAO Shouting* (高守亭)

LASG, Institute of Atmospheric Physics, Chinese Academy of Sciences, Beijing 100029

Received January 10, 2003

ABSTRACT

By using PSU/NCAR MM5 mesoscale model, a 60-h simulation is performed to reproduce a frontal cyclogenesis over the Western Atlantic Ocean during March 13 — 15 1992. The model reproduces well the genesis, track and intensity of the cyclone, its associated thermal structure as well as its surface circulation. The major cyclone (M) deepens 45 hPa in the 60-h simulation and 12 hPa in 6 hours from 36 h to 42 h (model time) and 27 hPa in 24 hours from 36 h to 60 h (model time). Cross-section and isentropic analysis tell us that the cyclogenesis is in very close relation with slantwise isentropic surfaces; the cyclone is always superposed on the core of neutral convective stability with nearly vertical isentropic surfaces, which coincides with what the theory of Slantwise Vorticity Development (SVD) says. Beginning with the theory of SVD, the development and propagation of the oceanic frontal cyclone are studied by using high-resolution model output in the context of slantwise isentropic surfaces. The results show that the frontal cyclone deepens rapidly by the interaction with the large-scale environment after occurring over the ocean with weak static stability; and the theory of SVD can well interpret the development and propagation closely related with slantwise isentropic surfaces. The downstream slantwise up-sliding movement along canting isentropic surfaces makes vorticities develop (USVD) under favorable condition ($\dot{C}_D < 0$, where C_D is SVD index), and results in the moving and development of the cyclone.

Key words: Up-sliding Slantwise Vorticity Development (USVD), oceanic frontal cyclogenesis

I. INTRODUCTION

The concept of explosive cyclogenesis was first put forward by Sanders and Gyakum in the 1980s (Sanders and Gyakum 1980). They defined the explosive cyclogenesis which has a deepening rate of $(24\sin\phi/\sin 60°)$ hPa or more in 24 hours (ϕ is the latitude of the cyclonic center) and is called "Bomb". This kind of extratropical cyclogenesis develops fast with rapid falling of central pressure in short time, acutely increasing wind speed near the cyclone and intense weathers. Bombs mainly occur over oceans with violent variation of intensity and often threaten navigations seriously. With the rapid development of economics and shipping and the urgent demands of operational predictions of oceanic cyclones, more comprehensive and closer studies should be done to investigate the

* This work was supported by the Innovation Project of Chinese Academy of Sciences under Grant No. KZCX3-SW-213 and "Outstanding Overseas Chinese Scholars" project of the Chinese Academy of Sciences under Grant No. 2002-1-2 and the National Key Program for Developing Basic Sciences (G1998040900-part 1).

© 1994-2010 China Academic Journal Electronic Publishing House. All rights reserved. http://www.cnki.net

development of explosive cyclones.

Early studies mainly focused on statistical analyses (Sanders and Gyakum 1980; Murty et al. 1983; Zhang and Chen 1992), recently the physical factors of explosive cyclogenesis have been discussed in-depth (Robert et al. 1996; Uccellini et al. 1985; Li and Ding 1989; Gao et al. 1990; Sun and Gao 1993; Gyakum et al. 1992; Marco et al. 1999). Yi and Ding (1989) summarized the recent studies on extratropical cyclones and discussed climatic characteristics, synoptic situations, various mechanisms and numerical simulations of explosive cyclogenesis. The results showed that explosive cyclogenesis has something to do with not only large-scale conditions but also oceanic conditions and large-scale planetary waves, and the northern side of the upper-level jet is the most favorable area for explosive cyclogenesis.

According to the theory of dynamic instability, baroclinic instability is treated as the chief starting-up mechanism for synoptic systems in middle latitudes (Anthes et al. 1983; Rogers and Bosart 1986). Some numerical simulations told that if there is no latent heat release, there will be no explosive cyclogenesis, that is, latent heat release is one of the key factors of explosive cyclogenesis (Macro et al. 1999; Xu and Zhou 1999). Starting from the viewpoint of dynamic features and energetics, Lu and Sun (1996) showed that the downward extending of the air with high potential vorticity in the upper troposphere is one of the important factors for explosive cyclogenesis. Rasmussen (1979) suggested that the potential instability caused when cold fronts move over warm underlying surface will lead to some processes similar to CISK, and further result in drastic development of cyclones. Emanuel (1979; 1983) pointed out that symmetric instability could be important to explosive marine cyclogenesis. Huang and Qin (1998) found that energy dispersion is one of the mechanisms for explosive cyclogenesis, and energetic fluxes over oceans are more important in early phases of cyclones than later phases (Huang et al. 1999; Xie et al. 1985; Du and Yu 1991; Kuo et al. 1991).

In spite of that much attention has been paid to frontal cyclones in recent years, case studies, especially numerical simulations on minute structures and evolutions of this kind of mesoscale system are scarce. There are no very concurrent statements about the relative contributions of all kinds of factors for cyclogenesis. And it is also scarce to investigate the evolutions in the context of slantwise isentropic surfaces. Based on the precise primitive equations, the theory of Slantwise Vorticity Development (SVD) was proposed to study the development of the vertical component of vorticities in a moist baroclinic atmosphere. According to the theory, vorticities are apt to develop near steep isentropic surfaces (Wu et al. 1995; Wu and Cai 1997; Wu and Liu 1998; 1999). Here by using PSU/NCAR MM5 mesoscale model, a simulation is performed to reproduce a frontal cyclogenesis and the evolution of the cyclone will be studied with the theory of SVD in the context of steep isentropic surfaces to better understanding of the mechanisms of this kind of cyclone and our prediction of the cyclones.

Next section provides a brief description of the main model features used for the present study and the model initialization and initial conditions. Section III examines the structure and evolution of the frontal cyclone from 0000 UTC 13 to 1200 UTC 15 March 1992. Section IV provides brief description of the theory of SVD and its deduction

© 1994-2010 China Academic Journal Electronic Publishing House. All rights reserved. http://www.cnki.net

(USVD). And the development and movement of the cyclone are discussed qualitatively and quantitatively based on the deduction in Section V. A theoretical model is given in Section VI; At last, a summary and concluding remarks are given in Section VII.

II. MODEL DESCRIPTION AND INITIALIZATION

The case mentioned in this paper has been studied before, the PSU/NCAR MM4 was used for a 60-h simulation of this case by Zhang et al. (1999a; b); in their study, the NCEP 2°×2° latitude-longitude global analysis was first interpolated to the model coarse mesh as a first guess and then enhanced with conventional rawinsonde, ship and buoy observations to form the initial conditions. Here an improved version of the PSU/NCAR three-dimensional, nonhydrostatic, nested-grid, mesoscale model (MM5) is used for the present study. The fundamental features of the model used include: (1) a two-way interactive nested-grid procedure (Fig. 1a); (2) use of the Kain-Fritsch cumulus parameterization scheme for the fine-mesh domain and the Anthes-type cumulus scheme for the coarse-mesh domain; (3) an explicit simple ice moisture scheme for both coarse and fine-mesh domains; and (4) the Blackadar high-resolution boundary-layer parameterization.

The nested-grid ratio is 1 to 3, with a fine-mesh length of 30 km and a coarse-mesh length of 90 km. The (x, y, δ) dimensions of the coarse and fine meshes are 89×75×23 and 139×109×23 respectively, and they are overlaid on a polar-stereographic map projection true at 60°N. The 24 δ-levels are 0.0, 0.05, 0.1, 0.15, 0.2, 0.25, 0.3, 0.35, 0.4, 0.45, 0.5, 0.55, 0.6, 0.65, 0.7, 0.75, 0.8, 0.85, 0.89, 0.93, 0.96, 0.98, 0.99 and 1.0. The use of an interactive two-way nested grid is helpful for solving the boundary problem of regional models. And the pressure at the top of the model atmosphere is 70 hPa.

The model is initialized at 0000 UTC 13 March 1992 (henceforth 00/13−00) with data

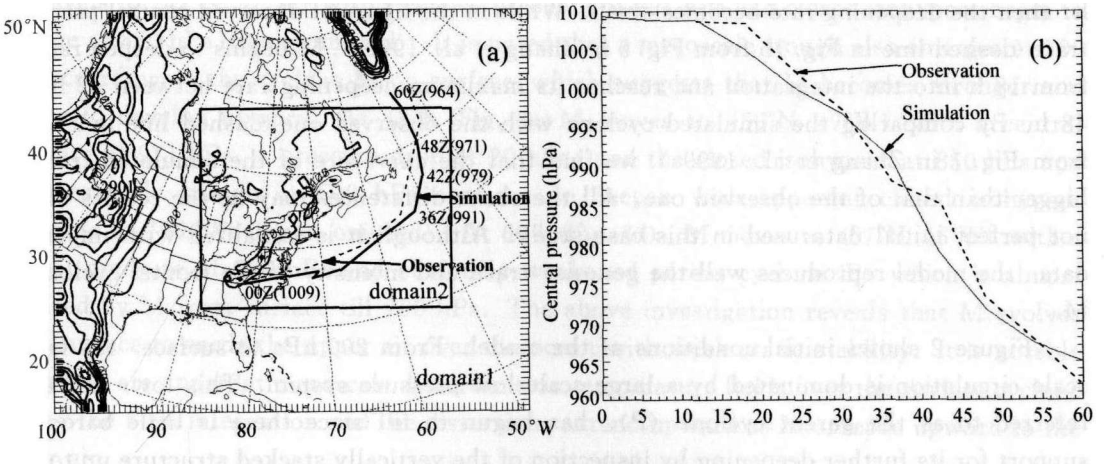

Fig. 1. Model domains, topography and tracks of the major cyclone (M) and its central pressure traces, solid lines for model results, and dashed lines for observations. (a) Model domains, topography and tracks; (b) Central pressure traces.

© 1994-2010 China Academic Journal Electronic Publishing House. All rights reserved. http://www.cnki.net

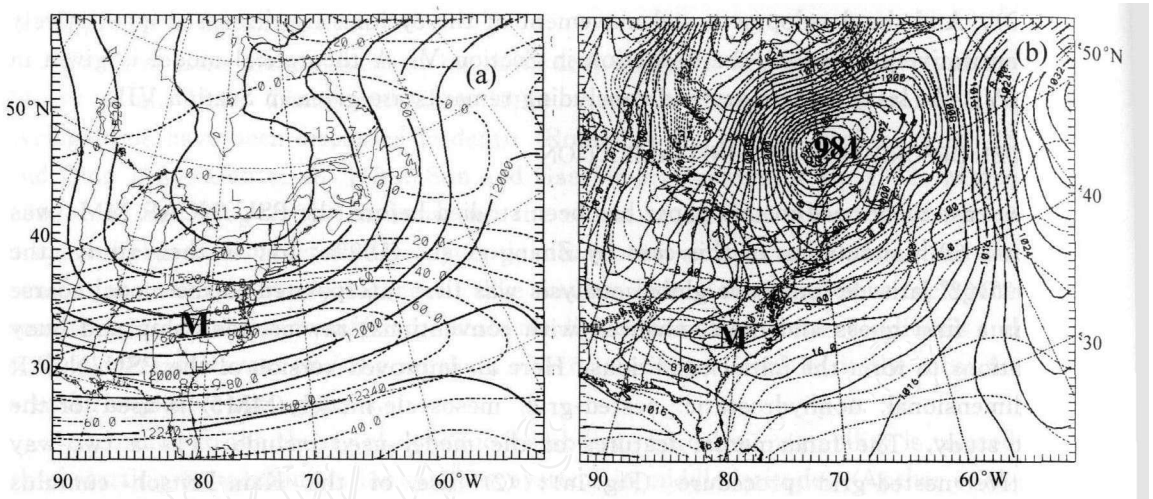

Fig. 2. Initial conditions of the model (00/13—00), letter "M" marks the center of the major cyclone. (a) 200 hPa height (solid) and isotachs of U component of wind (dashed) with speeds>60 m/s shaded; (b) sea-level pressure (solid) and surface temperature (dashed).

from the NCEP 2.5°×2.5° latitude-longitude global re-analysis and 1°×1° latitude-longitude global weekly averaged sea-surface temperature (SST, for short-time simulations, the effect of SST is not very important). The model domains, topography and the simulated track of the major cyclone (henceforth M) are shown in Fig. 1a (solid line), and the simulated central pressure trace of M is shown in Fig. 1b (solid line). M deepens altogether 45 hPa in the 60-h integration. It deepens 12 hPa in 6 hours from 36 h to 42 h into the integration (model time, hereafter all times refer to model time except special declarations) and 27 hPa in 24 hours from 36 h to 60 h, which has come to the criteria of explosive cyclogenesis (Sanders and Gyakum 1980). M begins to deepen rapidly at 12 h into the integration and reaches its maximum deepening rate between 36 h and 42 h; then the deepening rate becomes small. While in the figure of observed central pressure trace (dashed line in Fig. 1b from Fig. 5 in Zhang et al. 1999a), M begins to deepen rapidly from 18 h into the integration and reaches its maximum deepening rate between 42 h and 48 h. By comparing the simulated cyclone with the observed one (dashed line in Fig. 1a from Fig. 1 in Zhang et al. 1999a), we find that the curvature of the simulated track is bigger than that of the observed one. All the above differences may be the results of the not perfect initial data used in this case study. Although it is initialized with imperfect data, the model reproduces well the genesis, track and intensity of the frontal cyclone of M.

Figure 2 shows initial conditions of the model. From 200 hPa to surface, the large-scale circulation is dominated by a large-scale low-pressure system. This low, hereafter referred to as the parent cyclone (P), has begun to fill since there is little baroclinic support for its further deepening by inspection of the vertically stacked structure up to 200 hPa (Fig. 2). At 200 hPa (Fig. 2a) there is a westerly jet streak core of 86.9 m/s to the south of the cyclonic center and relatively weak wind in the center, to the northeast of which there is an easterly maximum value (−13.7 m/s). At 500 hPa (figure omitted) P is

© 1994-2010 China Academic Journal Electronic Publishing House. All rights reserved. http://www.cnki.net

located at (49°N, 71°W) to the southwest of which there is a southwest-northeast oriented short-wave trough with weaker temperature advection. The cyclonic circulation P is situated at (51°N, 71°W) at 850 hPa (figure omitted). There are cold advection behind the short-wave trough and warm advection before the trough, and the trough has a similar orientation to the Applachians and to the northwest of the Mountains. On the maps of sea level pressure (SLP) and surface temperature (Fig. 2b), the parent cyclone (P) lies at (52°N, 70°W) with a central pressure of 981 hPa, and the major cyclone (M) which appears as a mesoscale trough now is located to the southeast of the Applachians near the cyclonic side of the core of the upper-level westerly jet streak (200 hPa). There are large pieces of baroclinic zones along the east coast of America and over the oceans to the east of America. The mesoscale trough (M) just lies beneath the upper-level positive vorticity advection and at the cyclonic side of the upper-level westerly jet streak, which is favorable for the development of M.

III. CASE SIMULATION

1. *Sea-Level and Upper-Level Circulation*

The mesoscale trough (M) moves offshore and forms its first closed isobar at 18 h into the integration, i. e., 1800 UTC 13 March 1992 (18/13 — 18, figure is omitted for economy of space) with a central pressure of 1005 hPa (37°N, 68°W). M travels eastward to (38°N, 63°W) with the large-scale steering flow with a central pressure drop of about 5 hPa in 6 hours (00/14 — 24, Fig. 3a); At 850 hPa (figure omitted) there appears apparent mesoscale trough according to the cyclone M on surface with favorable cold and warm advections for further development of the trough; And at 700 hPa (figure omitted) there is corresponding favorable temperature structure helpful for the development of M though no apparent mesoscale trough is available. The parent cyclone (P) now moves northeastward to (57°N, 65°W) with a central pressure of 985 hPa. At 36 h into the integration (Fig. 3b), M travels to (42°N, 52°W) with a central pressure of 991 hPa and closed isohypses begin to emerge at 850 hPa (figure omitted). It is noted that a mesoscale trough also emerges at 700 hPa according to the cyclone M on surface, which suggests that M becomes stronger and begins to develop upward. At 48 h (Fig. 3c) M moves to (50°N, 47°W) with a central pressure of 971 hPa, a pressure drop of 20 hPa; and the closed isohypses at 850 hPa and the mesoscale trough at 500 hPa continue to deepen with apparent closed isohypses emerging at 700 hPa (figure omitted). At 60 h (Fig. 3d), M moves to (57°N, 45°W) with a central pressure of 964 hPa and obviously weakened parent cyclone (P) which is almost replaced by M from surface till 700 hPa. The above investigation reveals that M evolves from surface towards the upper air over the ocean with weak static stability. It is notable that there are apparent mesoscale distortions on temperature fields over the surface cyclone during the 60-h integration and the distortions extend upward as M spreads upward to the upper air.

To further verify the simulation, the simulated upper-level circulations at 42 h are analysed (figures omitted). At 200 hPa there is a westerly jet streak core of 67.6 m/s, a nearly 20 m/s drop from the initial time; the easterly maximum value decreases rapidly

© 1994-2010 China Academic Journal Electronic Publishing House. All rights reserved. http://www.cnki.net

(−0.572 m/s) and the parent cyclone (P) fills distinctly. At 500 hPa, there emerges a distinct mesoscale trough, together with which, the low at 850 hPa and the surface cyclone (at 46°N, 48°W with a central pressure of 979 hPa,), a proximate vertical structure is formed. The parent cyclone lies at (56°N, 63°W) with a central pressure of 986 hPa. Specially, there exists coincident apparent mesoscale temperature structures from surface to 500 hPa related to M, which, along with which, the large-scale temperature structure, has great impact on the future development of M.

The above analysis reveals that M is initiated in favorable large-scale circulations. After that, the large-scale circulations are modified by being overlaid on with self-organized mesoscale circulations, and on the contrary the modified large-scale circulations provide profitable conditions for the future movement and development of M.

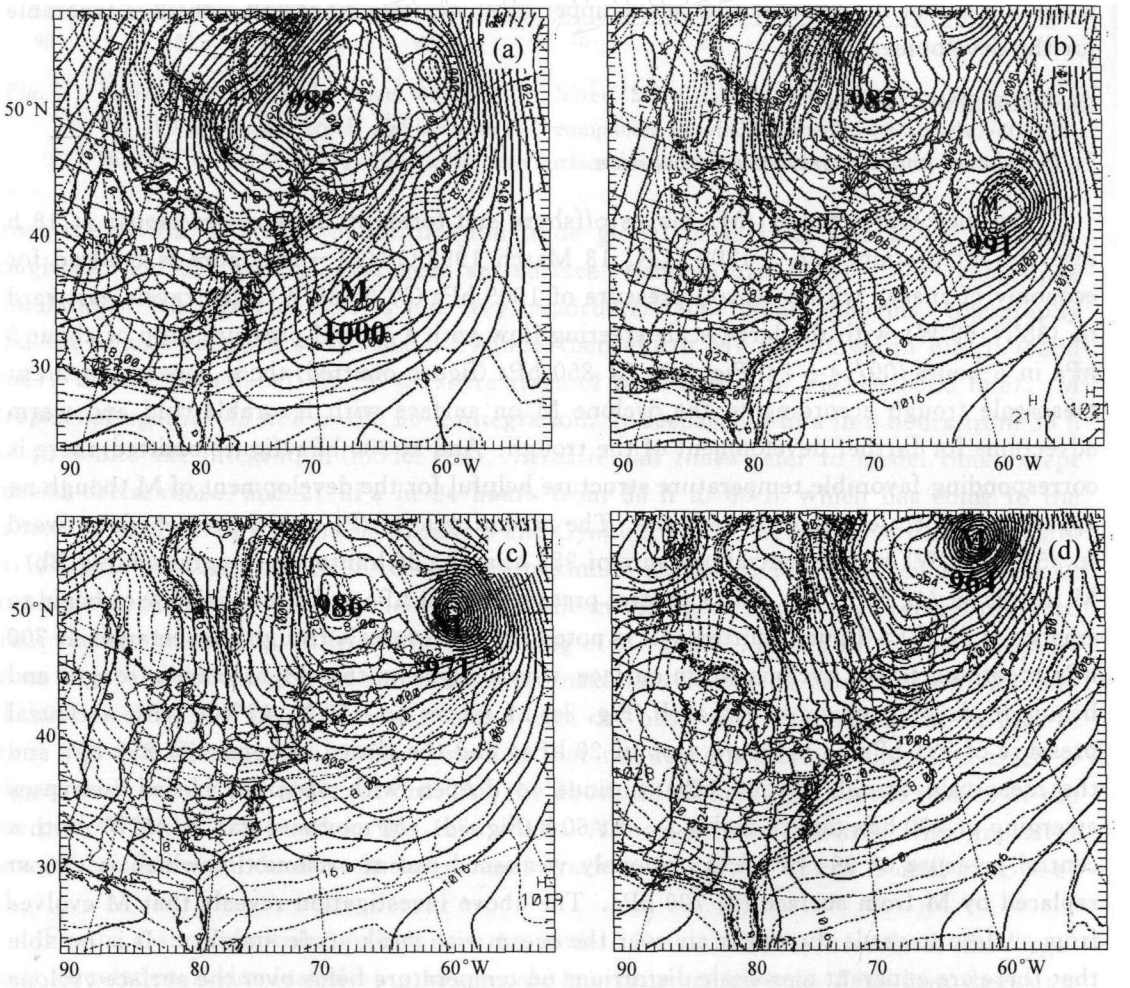

Fig. 3. Sea-level pressure (solid) and surface temperature (dashed), letter "M" marks the center of the major cyclone. (a) 24 h; (b) 36 h; (c) 48 h and (d) 60 h;

© 1994-2010 China Academic Journal Electronic Publishing House. All rights reserved. http://www.cnki.net

2. *Cross-Section and Isentropic Analysis*

From the above study, we know that M interacts with the large-scale circulations and then develops rapidly. An inspection of Fig. 3 and corresponding height maps at 700 and 850 hPa reveals that M always evolves along the concentrated isotherms over the ocean with weak static stability and M just lies in the area with stronger gradients of temperature. Then what does this look like in cross-sections? The east-west oriented cross-sections of potential temperature and equivalent potential temperature across the center of M at 42 h into the integration are shown in Fig. 4. It is obvious that not only isentropes but also moist isentropes are very slant and there are apparent vertical motions near the steep isentropics where vortexes are most likely to develop (according to the study of Wu and Liu (1999), when an air parcel moves along a slantwise isentropic surface, vorticities are apt to develop rapidly along the slantwise surface), and M just evolves along slant isentropic surfaces (seen from the surface pressure in Fig. 4). It is also notable that in Fig. 4b the center of M is superposed not on the center of convective unstable area but on the center of proximate neutral convective stability with slantwise moist isentropic surfaces. It is clear that the evolution of M must have something to do with slantwise isentropic surfaces.

The pressure and relative vorticity on 288 K isentropic surface are calculated and analyzed. The 288 K isentropic surface looks like an inverted "bowl" with lower pressure in the middle, higher one outside, concentrated isobars at the edge, which means

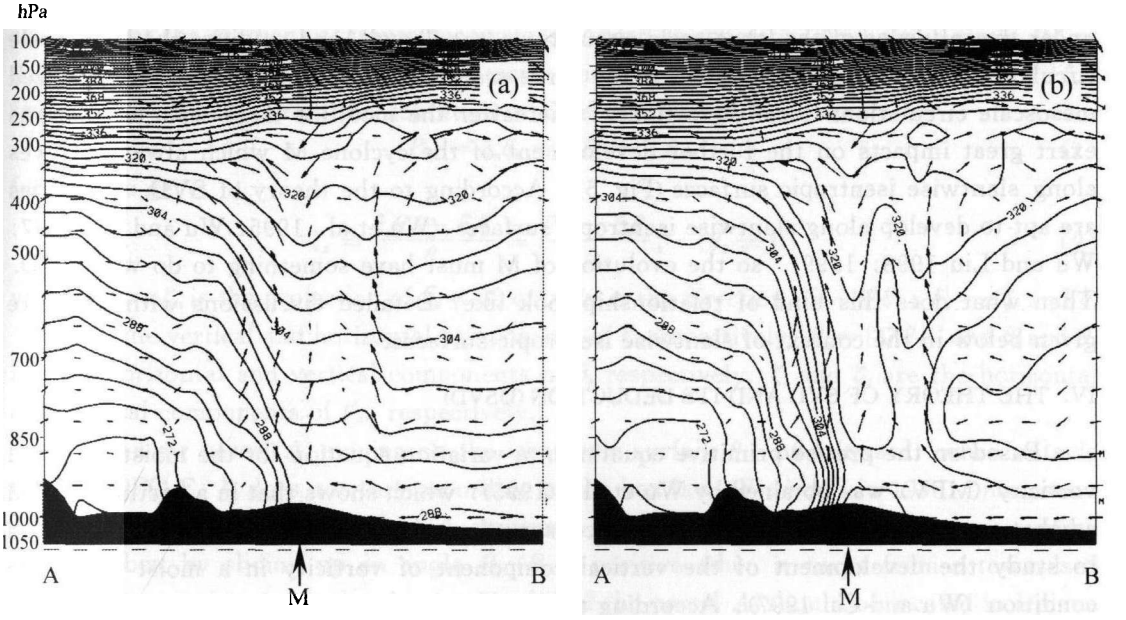

Fig. 4. Vertical cross-sections of (equivalent) potential temperature (solid every 4 K), superposed with along-plaoe wind vectors, which is taken across the centre of M at 42 h into the integration (18/14—42) from A (West) to B (East). Shaded area denotes surface pressure, the scales of horizontal and vertical motions are m/s and hPa/s respectively. (a) potential temperature; (b) equivalent potential temperature.

© 1994-2010 China Academic Journal Electronic Publishing House. All rights reserved. http://www.cnki.net

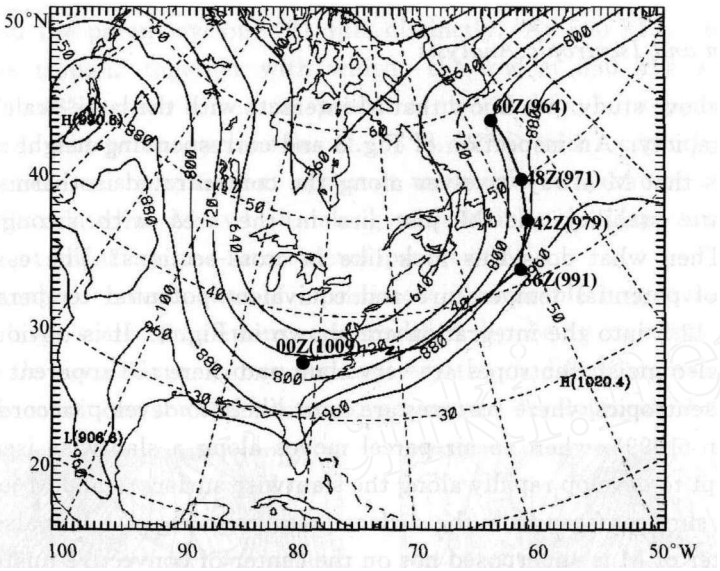

Fig. 5. Pressure (every 80 hPa, averaged in 60 hours) and simulated tracks of M on 288 K isentropic surface. Solid circles denote the positions of surface cyclone.

isentropic surfaces are very slant at the edge of the "bowl" (figures omitted). Centers of relative vorticities always evolve along the slantwise edge of the "bowl". During the whole evolution of the frontal cyclone, the inverted "bowl" does not change its shape except for some local distortions (Fig. 5). This is absolutely concurrent with the results from the above discussions of temperature maps and cross-sections. In fact, M develops and moves under the influence of the large-scale circulations (the "bowl") and modifies the large-scale circulations by interactions between the large-scale circulations and the self-organized mesoscale circulations (local distortions); thereafter the modified large-scale circulations exert great impacts on the further development of the cyclone M which always evolves along slantwise isentropic surfaces (Fig. 5). According to the theory of SVD, vorticities are apt to develop along slantwise isentropic surfaces (Wu et al. 1995; Wu and Cai 1997; Wu and Liu 1998; 1999), so the evolution of M must have something to do with SVD. Then what does this kind of relationship look like? Detailed discussions with SVD are given below in the context of slantwise isentropic surfaces.

IV. THE THEORY OF SVD AND ITS DEDUCTION (USVD)

Based on the precise primitive equations, a variation equation for the moist potential vorticity (MPV) was obtained by Wu et al. (1995), which shows that in a frictionless and adiabatic saturated atmosphere, MPV is conserved, and the theory of SVD was proposed to study the development of the vertical component of vorticity in a moist baroclinic condition (Wu and Cai 1997). According to the theory, vorticities are apt to develop near steep isentropic surfaces. Thereafter a new form of vertical vorticity equation was also produced from the definition of MPV and the MPV equation (Wu and Liu 1998). Compared with the traditional vorticity equation, the new equation has many advantages and is more applicable for diagnosis (Wu and Liu 1999).

Some researchers showed that up-sliding slantwise motions are always observed

© 1994-2010 China Academic Journal Electronic Publishing House. All rights reserved. http://www.cnki.net

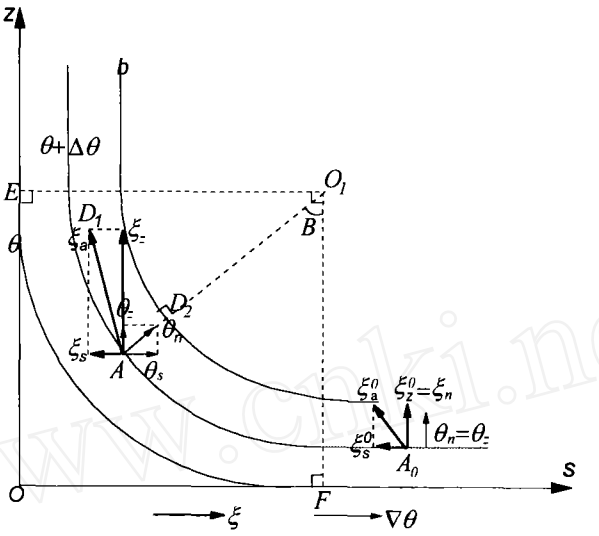

Fig. 6. Schematic diagram of up-sliding slantwise vorticity development.

during the development and movement of oceanic frontal cyclones (Zhang et al. 1999a; 1999b), which actuates us to improve the theory of SVD to be suitable for this situation. Then the theory of up-sliding slantwise vorticity development (USVD) is proposed here and used in the study of the oceanic frontal cyclone M. The USVD is described in Fig. 6, in which we assume that the parallel isentropic surfaces are horizontal or perpendicular outside the box OFO_1E, but are bent as circles inside the box. For simplicity, we further assume that the gradient of isentropic surfaces $\Delta\theta=\theta_n$ is constant. And also a circle "b" is defined, which is coaxial with the isentropic surfaces and keeps a constant distance $|\xi_n|$ from surface $\theta+\Delta\theta$. From the definition of Ertel PV, we get

$$P_E = \xi_n\theta_n = \xi_s\theta_s + \xi_z\theta_z, \tag{1}$$

further we get,

$$\xi_z = \frac{\xi_n\theta_n - \xi_s\theta_s}{\theta_z} = \frac{P_E - \xi_s\theta_s}{\theta_z}, \quad (\theta_z \neq 0) \tag{2}$$

where $\xi_n=\alpha\zeta_n$ is the projection of $\boldsymbol{\xi}_a=\alpha\boldsymbol{\zeta}_a$ on $\boldsymbol{n}$ ($\boldsymbol{n}$ is the direction of $-\nabla\theta$); $\xi_z=\alpha\zeta_z$ and $\xi_s=\alpha\zeta_s$ are the vertical and horizontal components of $\boldsymbol{\xi}_a$ respectively; $\theta_n=|\nabla\theta|$, and θ_s and θ_z are the horizontal and vertical components of θ_n respectively. ζ_s and ζ_z are the horizontal and vertical components of $\boldsymbol{\zeta}_a$, respectively.

For an air parcel A_0 moving on the isentropic surface $\theta+\Delta\theta$ leftward, when outside the box OFO_1E, ζ_z does not vary according to the box law (Wu and Liu 1998), no matter what $\xi_s=\alpha\zeta_s=\alpha\partial V_m/\partial z$ is. When A_0 continues to move leftward on the isentropic surface into the box by sliding up an angle B (B is positive when it turns from-z towards-S clockwise) to point A, the head point D_1 of $\boldsymbol{\zeta}_a$ of the parcel A_0 should be located in a plane D_1D_2 which is an externally tangential plane to circle "b" at point D_2 as shown in Fig. 6 according to the circumscribed plane law (Wu and Liu 1998). In Fig. 6 it is found that

$$\tan B = \frac{\theta_s}{\theta_z}, \quad \left(-\frac{\pi}{2} < B < \frac{\pi}{2}\right) \tag{3}$$

and, $\boldsymbol{n}\cdot\boldsymbol{k}>0$, then

© 1994-2010 China Academic Journal Electronic Publishing House. All rights reserved. http://www.cnki.net

$$\cos B = \frac{\theta_z}{\theta_n} > 0. \tag{4}$$

Introducing them into Eq. (2), we get

$$\xi_z = \frac{\xi_n}{\cos B} - \xi_s \tan B, \qquad \left(|B| \neq \frac{\pi}{2} \right). \tag{5}$$

In the Northern Hemisphere in the case of cyclogenesis, $\xi_n > 0$. If the following condition is satisfied:

$$C_D = \frac{\xi_s \theta_s}{\theta_z} < 0. \tag{6}$$

Equation (5) could be rewritten as

$$\xi_z = \frac{\xi_n}{\cos B} + |\xi_s \tan B|, \qquad \left(|B| \neq \frac{\pi}{2} \right), \tag{7}$$

where ξ_z increases with increasing $|B|$. When Eq. (6) is met (when point A_0 is outside the box, $\theta_s = 0$, so originally C_D equals 0. Then Eq. (6) is equivalent to $\dot{C}_D < 0$), the vertical component of absolute vorticity of parcel A_0 should grow, and when the isentropic surfaces are sharply steep, ξ_z can become very big. Because the development of vorticity is due to the up-sliding of the air parcel along a slantwise isentropic surface, it can be referred as up-sliding slantwise vorticity development (USVD). Upon applying the total derivative to both sides of Eq. (2), a new form of vertical vorticity equation for dry air can be obtained as

$$\frac{D\zeta_z}{Dt} + \beta v + (f + \zeta_z) \nabla \cdot \boldsymbol{V} = \frac{1}{\alpha} \frac{D}{Dt} \left(\frac{P_E}{\theta_z} - C_D \right), \quad \theta_z \neq 0 \tag{8}$$

where P_E is Ertel PV, $C_D = \frac{\xi_s \theta_s}{\theta_z}$ is dry SVD index, θ_z is the vertical component of the gradient of potential temperature.

If moist air is studied, the corresponding equation for moist air could be obtained as

$$\frac{D\zeta_z}{Dt} + \beta v + (f + \zeta_z) \nabla \cdot \boldsymbol{V} = \frac{1}{\alpha} \frac{D}{Dt} \left(\frac{P_M}{\theta_{ez}} - C_M \right), \quad \theta_{ez} \neq 0 \tag{9}$$

where P_M is MPV, $C_M = \frac{\xi_s \theta_{es}}{\theta_{ez}}$ is moist SVD index accordingly and θ_{ez} is the vertical component of the gradient of equivalent potential temperature.

V. SLANTWISE VORTICITY DEVELOPMENT

1. *Case Qualitative Diagnosis of USVD*

The above studies show that M is initiated and evolves over the ocean with weak static stability and its evolution could be explained with the theory of USVD. And as we know, if letting USVD hold, two prerequisites must be satisfied: one is steep isentropic surface; the other is slantwise motion (up-sliding or down-sliding). The first one has been proved to be true in the analysis of vertical cross-sections and the second one will be checked below.

Isentropic analysis is adopted here for the shape and declivity of isentropic surfaces can be expressed explicitly on isentropic surface maps (the distribution of isobars on isentropic surface maps tells the shape and steepness of isentropic surfaces; lower pressure

© 1994-2010 China Academic Journal Electronic Publishing House. All rights reserved. http://www.cnki.net

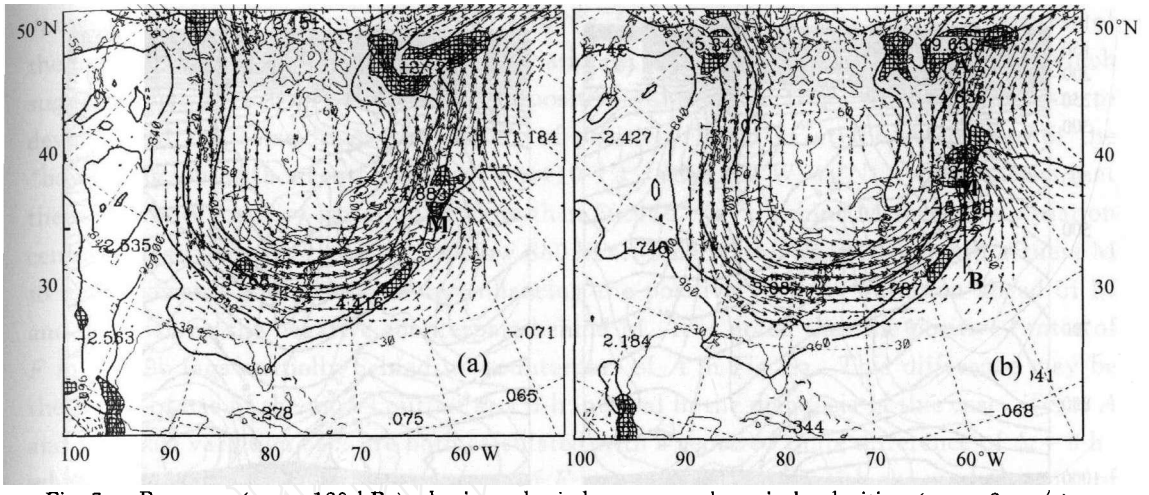

Fig. 7. Pressure (every 120 hPa), horizontal wind vectors and vertical velocities (every 2 cm/s) on 288 K isentropic surface at integration hour 36 h (a) and 42 h (b), and shading denotes vertical velocities >2 cm/s; the shortest vector denotes 9.97 m/s (a), 10.0 m/s (b), and the longest vector denotes 29.7 m/s (a), 29.8 m/s (b).

denotes higher isentropic surface while higher pressure denotes lower surface and the more concentrated the isobars are, the steeper the isentropic surfaces are). Horizontal wind vectors and vertical velocities are shown in Fig. 7 on 288 K isentropic surface at 36 h and 42 h into the integration (the superposition of these two fields denotes slantwise motions along isentropic surfaces), where bold and thin solid lines denote isobars and vertical velocities on isentropic surfaces respectively, and vertical velocities above 2 cm/s are shaded. The cyclonic center, like the surface cyclone M, also lies near steep isentropic surfaces (the edge of the inverted "bowl"). The cyclonic circulations ahead of M flow from higher pressure to lower one and are superposed with positive vertical velocities, which means that there exist slantwise up-sliding motions (this also can be proved in the above discussion of vertical cross-sections); and at the same time, there exist slantwise down-sliding motions behind M correspondingly. Therefore both of the two prerequisites mentioned above are satisfied in this case. It is noticeable that there are apparent distortions of isobars near the cyclonic circulation, which is the results of interactions between the large-scale circulations and the self-organized mesoscale circulations (Fig. 7). And the modified distributions of isobars, together with the up-sliding motions ahead of M, provide very favorable conditions for the arising of USVD.

Vertical cross-sections of potential temperature (bold, every 4 K) superposed with along-plane horizontal wind velocities (thin, every 4 m/s) taken along line AB in Fig. 7b are shown in Fig. 8. At 36 h into the integration (Fig. 8a), there are corresponding vertical shears of horizontal wind ahead of the cyclone M with a direction pointing out from the paper accompanying the slantwise up-sliding motions mentioned above. In this kind of situation the vertical shears equal ξ_s and their directions should be in the direction of $-\boldsymbol{S}$ in Fig. 6, i.e., $\xi_s<0$; and in general $\theta_s>0$ and $\theta_z>0$ in this case (Fig. 6), thus $C_D=\frac{\xi_s\theta_s}{\theta_z}<0$. When an air parcel slides up along slantwise isentropic surfaces ahead of the cyclone M,

© 1994-2010 China Academic Journal Electronic Publishing House. All rights reserved. http://www.cnki.net

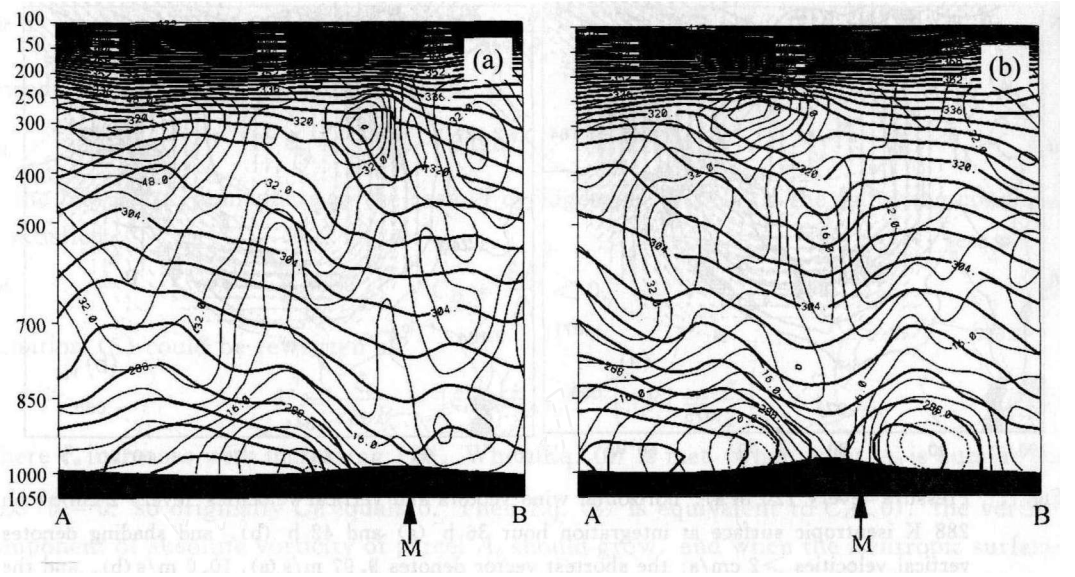

Fig. 8. Vertical cross-sections of potential temperature (bold, every 4 K) at integration hour 36 h (a) and 42 h (b), superposed with along-plane horizontal wind velocities (thin, every 4 m/s), which is taken along line AB in Fig. 7b. Shaded area denotes surface pressure and the letter "M" denotes the surface cyclone.

$\dot{C}_D<0$, (when an air parcel moves horizontally, as seen in Fig. 6, $\theta_s=0$, and then $C_D=0$); then USVD will arise ahead of M (Fig. 8a) and positive relative vorticities will develop. At 42 h (Fig. 8b) USVD will also arise in front of the cyclone M.

The above analysis reveals that in this case the self-organized mesoscale circulations interact with the large-scale circulations and then USVD arises ahead of the cyclone M, which actuates the cyclone to move and develop rapidly. It is noted that negative relative vorticities develop behind M (from Fig. 7, there are down-sliding motions behind the cyclone, so negative relative vorticities will develop there according to Figs. 6 and 8), thus as a whole, the cyclone M will develop and move on along slantwise isentropic surfaces.

2. *Case Quantitative Diagnosis of USVD with the New Form of Vertical Vorticity Equation*

To further understand the impacts of USVD on the movement and development of M, a simple diagnosis will be performed with the new form of vertical vorticity equation as below

$$\frac{\partial \zeta_z}{\partial t} + \boldsymbol{V} \cdot \nabla \zeta_z + \beta v + (f + \zeta_z) \nabla \cdot \boldsymbol{V} = \frac{1}{\alpha} \frac{\mathrm{d}}{\mathrm{d}t}\left(\frac{P_E}{\theta_z}\right) - \frac{1}{\alpha} \frac{\mathrm{d}C_D}{\mathrm{d}t}, \tag{10}$$

where the first term on the left side is the local variation of relative vorticity (A term) and the last term on the right side ($-\frac{1}{\alpha}\frac{\mathrm{d}C_D}{\mathrm{d}t}$) is the index of SVD ($F$ term). For simplification, here only these two terms are diagnosed.

The local variation of relative vorticity (A term, thin lines) on 288 K isentropic surface at 36 h into the integration is given in Fig. 9a, where bold lines denote isobars and the letter "M" denotes the surface cyclone. In Fig. 9a, bigger local variations of relative vorticities lie always at the edge of the inverted "bowl", especially in the east part of the

© 1994-2010 China Academic Journal Electronic Publishing House. All rights reserved. http://www.cnki.net

"bowl". There is a local variation of $82\times10^{-10}s^{-2}$ near (48°W, 46°N), i.e., the position of the surface cyclone at 42 h and a local variation of about $-40\times10^{-10}s^{-2}$ behind M, which suggests that M will move towards the positive variation in front of it and continue to develop. At the same time, the centers of positive F also lie at the steep edge of the "bowl" (Fig. 9b) with a center of above $66\times10^{-10}s^{-2}$ near (50°W, 44°N), which means that there will be a vorticity variation of more than $60\times10^{-10}s^{-2}$; behind M there is a variation center of less than $-40\times10^{-10}s^{-2}$ below 880 hPa. This reveals that USVD will actuate M to move towards the positive F by enhancing the positive vorticity variation ahead of M and diminishing the negative counterpart behind M. It is noted that the positive center of F in Fig. 9b lags spatially behind its counterpart of A in Fig. 9a. This difference may be the result of use of the model output at a 6-h interval in the diagnosis of this case. Term A and the local variation of F are both calculated with a centered finite difference of $\Delta t=6$ h, while the advective and convective parts of F term are calculated with the model output of a certain moment. At 42 h into the integration (Figs. 9c, 9d), both of the variations of A

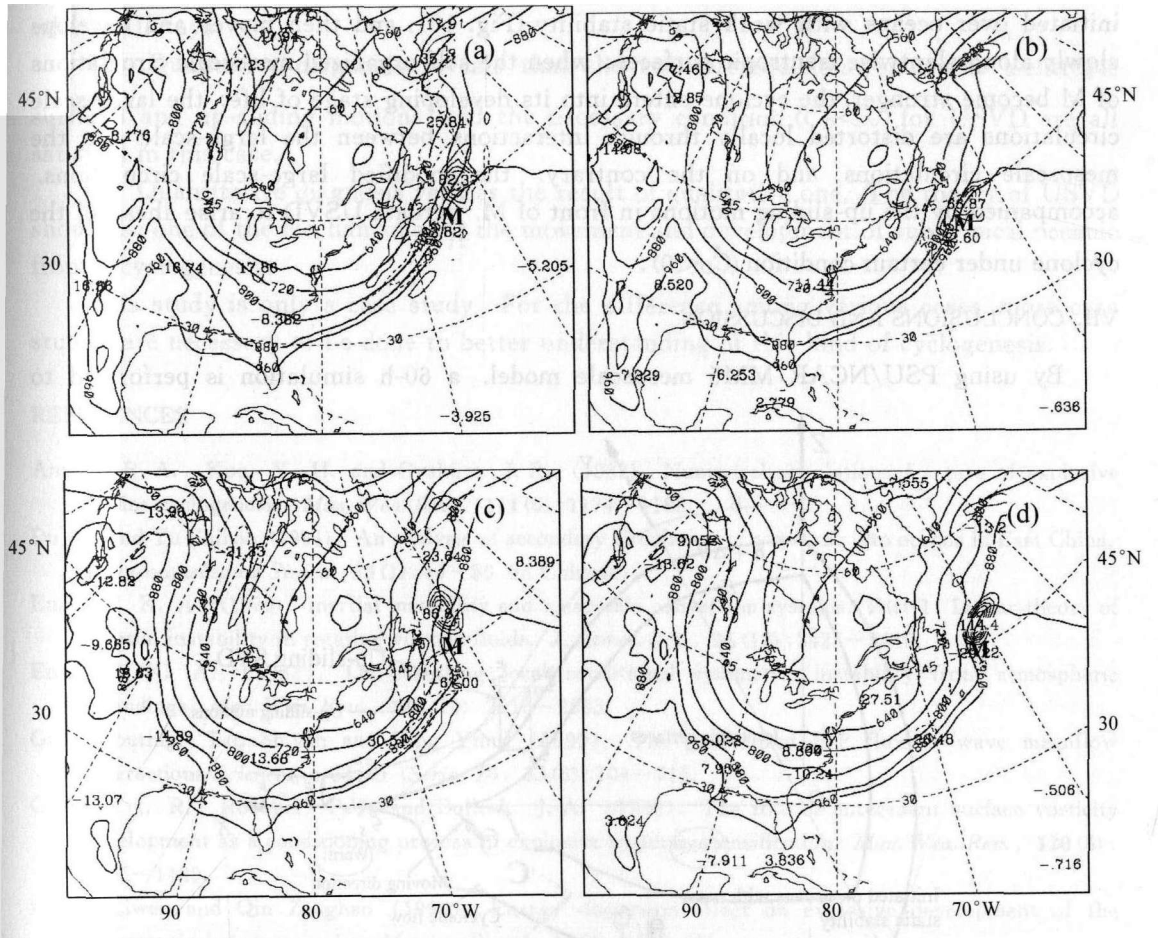

Fig. 9. Local variation of relative vorticity (a, c, thin, every $15\times10^{-10}s^{-2}$) and index of SVD (b, d, thin, every $15\times10^{-10}s^{-2}$) on 288 K isentropic surface at integration hour 36 h (a, b) and 42 h (c, d).

© 1994-2010 China Academic Journal Electronic Publishing House. All rights reserved. http://www.cnki.net

and F become more violent, while both of the centers of A and F lie still near slantwise isentropic surfaces.

It is noted that term F is equivalent to the term of tan$B$ in Eq. (5) and the first term on the right side in Eq. (10) is equivalent to the first term on the right side in Eq. (5), and that when $C_D<0$, all the terms on the right side of Eq. (10) have positive contributions to the development of vorticity according to Eq. (7). Therefore though F term is calculated here only, in fact the whole contribution of USVD is involved.

The above quantitative analysis suggests that USVD should be one of the mechanisms for movements and developments of subtropical oceanic frontal cyclogenesis.

VI. THEORETICAL MODEL

The theoretical model of this case is presented in Fig. 10, where θ and $\theta+\Delta\theta$ are two isentropic surfaces. The surface cyclone, track and self-organized mesoscale circulations are also presented (Fig. 10). The physical meaning of the plane XOZ and the other meteorological symbols in Fig. 10 have the same meaning as the symbols in Fig. 6. M is initiated over oceans with weak static stability (Fig. 10), and then moves and develops slowly along slantwise isentropic surfaces; when the self-organized mesoscale circulations of M become stronger, the cyclone enters into its developing stage of life; the large-scale circulations are distorted locally through interactions between the large-scale and the mesoscale circulations, and on the contrary, the modified large-scale circulations, accompanied by the up-sliding motions in front of M, actuate USVD to arise ahead of the cyclone under certain condition ($\dot{C}_D<0$).

VII. CONCLUSIONS AND DISCUSSION

By using PSU/NCAR MM5 mesoscale model, a 60-h simulation is performed to

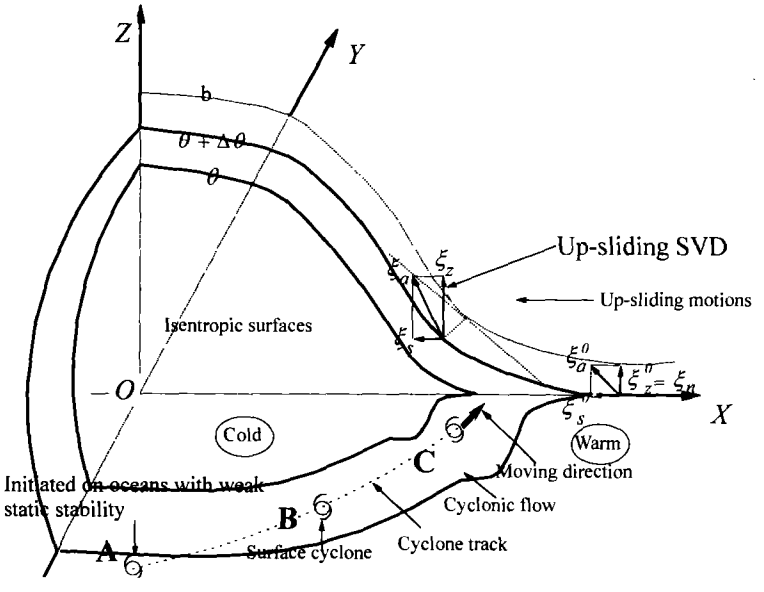

Fig. 10. Case theoretical model.

© 1994-2010 China Academic Journal Electronic Publishing House. All rights reserved. http://www.cnki.net

reproduce a frontal cyclogenesis over the Western Atlantic Ocean during March 13—15, 1992. Beginning with the theory of SVD, the genesis, development and propagation are studied by using high-resolution model output in the context of slantwise isentropic surfaces. And inspiring results are received:

(1) The model reproduces well the genesis, track and intensity of the cyclone, its associated thermal structure as well as its surface circulation. The major cyclone (M) deepens 45 hPa in the 60-h simulation and 12 hPa in 6 hours from 36 h to 42 h (model time) and 27 hPa in 24 hours from 36 h to 60 h (model time).

(2) M is initiated under favorable large-scale circulations. After that, the large-scale circulations are modified by superposition with the self-organized mesoscale circulations; and on the contrary, the modified large-scale circulations provide favorable conditions for the further movement and development of the cyclone.

(3) Cross-section and isentropic analysis tell us that the cyclogenesis is closely related to slantwise isentropic surfaces; the cyclone is always superposed on the core of proximate neutral convective stability with nearly vertical isentropic surfaces, which coincides with what SVD says.

(4) Qualitative diagnosis reveals that the two prerequisites (slantwise isentropic surfaces and up-sliding motions) and the necessary condition ($\dot{C}_D < 0$) for USVD are all satisfied in this case.

(5) Quantitative diagnosis verifies the result of qualitative one. The theory of USVD should be one of the mechanisms for the movement and development of subtropical oceanic frontal cyclogenesis.

This study is only a case study. For the difference among various cases, more case studies are necessary to be done to better understanding of this kind of cyclogenesis.

REFERENCES

Anthes, R. A., Kuo, Y. H. and Gyakum, J. R. (1983), Numerical simulationsof a case of explosive marine cyclogenesis. *Mon. Wea. Rev.*, **111** (6) : 1174—1188.

Du Jun and Yu Zhihao (1991), An analysis of secondary circulation of a cyclone into oceans in East China, *Acta Oceanologica Sinica*, **13** (1) : 43—50 (in Chinese).

Emanuel, K. A. (1979), Inertial instability and mesoscale convection systems, Part 1: Linear theory of inertial instability in rotating viscous fluids, *J. Atmos. Sci.*, **36** (12) : 2425—2449.

Emanuel, K. A. (1983), On assessing local conditional symmetric instability from atmospheric soundings, *Mon. Wea. Rev.*, **111** (10) : 2016—2033.

Gao Shouting, Tao Shiyan and Ding Yihui (1990), The generalized E-P flux of wave meanflow interactions *Sciences in China (Series B)*, **33** (6) : 704—715.

Gyakum, J. R., Roebber, P. J. and Bullock, J. A. (1992), The role of antecedent surface vorticity development as a conditioning process in explosive cyclone intensification, *Mon. Wea. Rev.*, **120** (8) : 1465—1489.

Huang Liwen and Qin Zenghao (1998), Energy dispersion effect on explosive development of the extratropical cyclones, *Acta Meteor. Sinica*, **12** (3) : 486—503.

Huang Liwen, Qin Zenghao, Wu Xiuheng and Zou Zaojian (1999), Numerical simulation and experiment study on explosive marine cyclones, *Acta. Meteor.. Sinica*, **57** (4) : 410—428 (in Chinese).

Kuo, Y. H., Reed, R. J. and Low-Nam, S. (1991), Effects of surface energy fluxes during the early

© 1994-2010 China Academic Journal Electronic Publishing House. All rights reserved. http://www.cnki.net

development and rapid intensification stages of seven explosive cyclones in the Western Atlantic, *Mon. Wea. Rev.*, **119** (2) : 457—476.

Kuo, Ying-Hwa, Shapiro, M. A. and Evelyn, G. Donall (1991), The interaction between baroclinic and diabatic processes in a numerical simulation of a rapidly intensifying extratropical marine cyclone, *Mon. Wea. Rev.*, **119** (2) : 368—384.

Li Changqing and Ding Yihui (1989), A diagnostic study of an explosively deepening oceanic cyclone over the Northwest Pacific ocean, *Acta Meteor. Sinica*, **47** (2) : 180—190 (in Chinese).

Lu Xiaoying and Sun Shuqing (1996), A study on the dynamic features and energy conversion of the development of explosive cyclones, *Scientia Atmos. Sinica*, **20** (1) : 90—100 (in Chinese).

Marco, L. Carrera, John, R. Gyakum and Zhang Da-Lin (1999), A numerical case study of secondary marine cyclogenesis sensitivity to initial error and varying physical processes, *Mon. Wea. Rev.*, **127** (5) : 641—660.

Murty, T. S., McBean, G. A. and McKee, B. (1983), Explosive cyclogenesis over the Northeast Pacific Ocean, *Mon. Wea. Rea.*, **111** (5) : 1131—1135.

Robert, L. M. et al. (1996), A diagnosis of a model-simulated explosively developing extratropical cyclone, *Mon. Wea. Rev.*, **124** (5) : 875—904.

Robert, W. et al. (1994), A diagnostic study of the early phases of sixteen western North-Pacific cyclones, *J. Met. Soc. Japan*, **72** (4) : 515—530.

Rogers, E. and Bosart, L. F. (1986), An investigation of explosively deepening oceanic cyclones, *Mon. Wea. Rev.*, **114** (4) : 702—718.

Sanders, F. and Gyakum, J. R. (1980), Synoptic dynamic climatology of the "Bomb", *Mon. Wea. Rev.*, **108** (10) : 1589—1606

Sun Shuqing and Gao Shouting (1993), The influence of the activity of cold wave in East Asia on the explosive cyclone at its down stream, *Acta. Meteor. Sinica*, **51** (3) : 304—314 (in Chinese).

Uccellini, L. W., Keyser. D., Brill, K. F. and Wash, C. H. (1985), The President's day cyclone of 18—19 February 1979: Influence of upstream trough amplification and associated tropopause folding on rapid cyclogenesis, *Mon. Wea. Rev.*, **113** (6) : 962—988.

Wu Guoxiong, Cai Yaping and Tang Xiaojing (1995), Moist potential vorticity and slantwise vorticity development, *Acta Meteor. Sinica*, **53** (4) : 387—405 (in Chinese).

Wu Guoxiong and Cai Yaping (1997), Vertical wind shear and down-sliding slantwise vorticity development, *Scientia Atmospherica Sinica*, **21** (3) : 273—281 (in Chinese).

Wu Guoxiong and Liu Huanzhu (1998), Vertical vorticity development owing to down-sliding at slantwise isentropic surface, *Dynamics of Atmospheres and Oceans*, **27**: 715—743.

Wu Guoxiong and Liu Huanzhu (1999), Complete form of vertical vorticity tendency equation and slantwise vorticity development, *Acta Meteor. Sinica*, **57** (1) : 1—13 (in Chinese).

Xie Liusen, Wang Binhua and Zuo Zhongdao (1985), A dynamic diagnostic study of the influence of Kuroshio current on the development of cyclones, *Acta Oceanologica Sinica*, **7** (2) : 154—164 (in Chinese).

Xu Yinlong and Zhou Mingyu (1999), Numerical simulations on the explosive cyclogenesis over the Kuroshio Current, *Advs. Atmos. Sci.*, **16** (1) : 64—75

Yi Qingju and Ding Yihui (1989), A study on the evolution of subtropical marine cyclones, *Scientia Atmospherica Sinica*, **13** (2) : 238—246 (in Chinese).

Zhang Peizhong and Chen Shoujun (1992), *Climatic Atlas of Subtropical Cyclones in Asia and the Pacific Ocean*, China Meteor. Press, Beijing (in Chinese).

Zhang D.-L., Radeva E., Gyakum J. (1999a), A family of frontal cyclones over the Western Atlantic Ocean. Part I : A 60-h simulation, *Mon. Wea. Rev.*, **127** (8) : 1725—1744.

Zhang D.-L., Radeva E., Gyakum, J. (1999b), A family of frontal cyclones over the Western Atlantic Ocean. Part II : Parameter studies *Mon. Wea. Rev.*, **127** (8) : 1745—1760.

© 1994-2010 China Academic Journal Electronic Publishing House. All rights reserved. http://www.cnki.net